AMERICAN SOCIETY FOR MICROBIOLOGY | Infection and Immunity

Immunology | Full-Length Text

IL-33-binding HpARI family homologues with divergent effects in suppressing or enhancing type 2 immune responses

Florent Colomb,[1] Adefunke Ogunkanbi,[1,2] Abhishek Jamwal,[3,4] Beverly Dong,[5,6] Rick M. Maizels,[7] Constance A. M. Finney,[5,6] James D. Wasmuth,[6,8] Matthew K. Higgins,[3,4] Henry J. McSorley[1]

AUTHOR AFFILIATIONS See affiliation list on p. 11.

ABSTRACT HpARI is an immunomodulatory protein secreted by the intestinal nematode *Heligmosomoides polygyrus bakeri*, which binds and blocks IL-33. Here, we find that the *H. polygyrus bakeri* genome contains three HpARI family members and that these have different effects on IL-33-dependent responses *in vitro* and *in vivo*, with HpARI1+2 suppressing and HpARI3 amplifying these responses. All HpARIs have sub-nanomolar affinity for mouse IL-33; however, HpARI3 does not block IL-33-ST2 interactions. Instead, HpARI3 stabilizes IL-33, increasing the half-life of the cytokine and amplifying responses to it *in vivo*. Together, these data show that *H. polygyrus bakeri* secretes a family of HpARI proteins with both overlapping and distinct functions, comprising a complex immunomodulatory arsenal of host-targeted proteins.

KEYWORDS IL-33, helminth, immunomodulation

IL-33 is an IL-1 family alarmin cytokine which is constitutively expressed by epithelial cells, where it is stored in cellular nuclei and released under conditions of damage and necrosis (1). Upon release, the active mature cytokine is rapidly oxidized, rendering it unable to bind to its receptor ST2 (2), limiting its ST2-dependent activity *in vivo* to the local milieu and to a short period of time after release. IL-33 acts as an initiator of allergic diseases, especially asthma, where both IL-33 and ST2 are genetically linked to disease heritability (3) and are targets for new biologic treatments (4, 5). IL-33 also plays a significant role in the expulsion of parasitic helminths, with deficiency or blockade of the IL-33 pathway resulting in increased parasite burden (1, 6, 7). Conversely, IL-33 can also have immunosuppressive effects, inducing regulatory T cells in the gut (8), and inflammatory effects, inducing IFN-γ production by IL-12-stimulated $CD8^+$ T cells (9). Thus, in different contexts, IL-33 responses can either increase or decrease susceptibility to parasitic helminths (10).

Parasitic helminth infection affects more than one billion people worldwide. The relationship between parasites and their hosts reflects co-evolutionary adaptation to host protective immune mechanisms which results in parasites' long persistence in the host (11, 12). Excretory-secretory (ES) products released from helminths contain a wide range of molecules which can modulate the host immune system, suppressing anti-parasitic immune responses and hence promoting parasite survival (13, 14). The murine intestinal parasite *Heligmosomoides polygyrus bakeri* (*Hpb*) is a prime example of this host-parasite dynamic. *Hpb* secretions contain the Alarmin Release Inhibitor (HpARI) and Binds Alarmin Receptor and Inhibits (HpBARI), both of which block the IL-33 pathway and suppress type 2 immune responses in mice (15, 16).

In our previous work, we identified HpARI, showing that it binds IL-33 and blocks type 2 immune responses (15), and used structural studies to demonstrate how this IL-33-ST2 inhibition is achieved (17). Here, we show that the *Hpb* genome encodes a family of three HpARI proteins: HpARI1, HpARI2, and HpARI3, with the original HpARI now renamed as

Editor De'Broski R. Herbert, University of Pennsylvania, Philadelphia, Pennsylvania, USA

Address correspondence to Henry J. McSorley, hmcsorley001@dundee.ac.uk.

Florent Colomb, Adefunke Ogunkanbi, and Abhishek Jamwal contributed equally to this article. Author order was decided by number of figures contributing to final draft.

The authors declare no conflict of interest.

See the funding table on p. 12.

Received 6 October 2023
Accepted 27 December 2023
Published 31 January 2024

HpARI2. We expressed and tested these proteins for their activity *in vitro* and *in vivo*, and unexpectedly found that HpARI3 enhances rather than suppresses IL-33 responses. This study indicates that *Hpb* products can both boost and suppress IL-33 responses.

MATERIALS AND METHODS

Mass spectrometry

The *Hpb* excretory/secretory products (HES) were prepared as described previously (18), and a 2 µg sample was used for mass spectrometry (MS) analysis. Triethylammonium bicarbonate (Sigma) and dithiothreitol (Merck Millipore) were added to final concentrations of 100 and 10 mM, respectively, and the sample was incubated at 70°C for 10 min. Alkylation was carried out by the addition of 20 mM iodoacetamide for 30 min in the dark. The sample was incubated overnight in the presence of 50 mM dithiothreitol, and 200 ng trypsin was added and incubated overnight at 37°C. Trifluoracetic acid (Fisher Scientific) at 10% sample volume was added, C18 clean-up was carried out using an Empore-C18 (Agilent) solid phase extraction cartridge, and dried samples were resuspended in 1% formic acid (Fisher Chemical).

Analysis of peptide readout was performed on a Q Exactive Plus Mass Spectrometer (Thermo Scientific) coupled to a Dionex Ultimate 3000 RS (Thermo Scientific). Liquid chromatography buffers used were as follows: buffer A [0.1% formic acid in Milli-Q water (vol/vol)] and buffer B [80% acetonitrile and 0.1% formic acid in Milli-Q water (vol/vol)]. An equivalent of 1.0 µg of peptides from each sample was loaded at 10 µL/min onto a µPAC trapping C18 column (PharmaFluidics). The trapping column was washed for 6 min at the same flow rate with 0.1% TFA and then switched in-line with a PharmaFluidics, 200 cm, µPAC nanoLC C18 column. The column was equilibrated at a flow rate of 300 nL/min for 30 min. The peptides were eluted from the column at a constant flow rate of 300 nL/min with a linear gradient from 2% buffer B to 5.0% buffer B in 5 min, from 5.0% buffer B to 35% buffer B in 125 min, and from 35% to 98% in 2 min. The column was then washed at 98% buffer B for 20 min and then washed at 2% buffer B for 20 min. Two blanks were run between each sample to reduce carry-over. The column was kept at a constant temperature of 50°C.

Q Exactive Plus Mass Spectrometer was operated in a positive ionization mode using an easy spray source. The source voltage was set to 2.90 kV, and the capillary temperature was 275°C. Data were acquired in Data Independent Acquisition (DIA) Mode as previously described (19), with little modification. A scan cycle comprised a full MS scan (m/z range from 345 to 1,155), resolution was set to 70,000, automatic gain control (AGC) target 1×10^6, and maximum injection time of 100 ms. MS survey scans were followed by DIA scans of dynamic window widths with an overlap of 0.5 Th. DIA spectra were recorded at a resolution of 17,500 at 200 m/z using an automatic gain control target of 2×10^5, a maximum injection time of 100 ms, and a first fixed mass of 100 m/z. Normalized collision energy was set to 27% with a default charge state set at 3. Data for both MS scan and MS/MS DIA scan events were acquired in profile mode.

Mass spectrometry data analysis: label-free analysis was performed in Maxquant (version 2.0.3.0) using the generated RAW files. Enzyme specificity was set to that of trypsin, allowing for cleavage N-terminal to proline residues and between aspartic acid and proline residues. Other parameters used were as follows: (i) variable modifications—oxidation (M), protein N-acetylation, gln → pyro-glu, deamidation (NQ), deoxidation (MW); (ii) fixed modifications—cysteine carbamidomethylation; (iii) database—in-house database; (iv) MS/MS tolerance—Fourier transform mass spectrometry (FT-MS) 10 ppm, FT-MSMS 0.06 Da; (v) maximum peptide length, 6; (vi) maximum missed cleavages, 2; (vii) maximum of labeled amino acids, 3; and (vii) false discovery rate, 1%. Match between runs (MBR) was set to true. Unique peptides were used for protein quantification.

Expression and purification of HpARI1-3 and HpBARI_Hom2

Proteins were expressed and purified using a protocol described previously (15, 16). Briefly, mammalian expression constructs carrying the C-terminal 6X-His-tagged gene of interest (HpARI1-3, HpBARI_Hom2, or ST2 ectodomain) were transfected individually into Expi293F cells (Thermo Fisher Scientific) using the Expifectamine transfection kit (Thermo Fisher Scientific). Cell supernatants were harvested 96 h post-transfection, and the expressed recombinant proteins were then captured from the filtered supernatants using Ni-NTA chromatography.

Surface plasmon resonance

To measure their binding affinities for mIL-33, the purified HpARI variants were first polished to remove aggregates using a Superdex S75 10/300 column in 1xPBS and chemically biotinylated using EZ-Link Sulfo-NHS-Biotin (Thermo Fisher Scientific) following the manufacturer's instruction. All surface plasmon resonance (SPR) experiments were carried out using a Biacore T200 instrument (GE Healthcare) using a CAP chip [Biotin CAPture kit (Cytiva)] in an SPR buffer containing 20 mM Tris-Cl, pH 8.0, 200 mM NaCl, 1 mg/mL salmon sperm DNA, and 0.05% Tween-20. Purified mIL-33 was equilibrated in the SPR buffer using a PD-5 column prior to the experiment. The sensor surface was first coated with oligonucleotide-coupled streptavidin following the manufacturer's instructions. Individual biotinylated HpARI variants were captured on different flow cells, followed by individual injections of a twofold concentration series of mIL-33 (50 to 0.195 nM for HpARI1 and HpARI2, and 200 to 0.781 nM for HpARI3) at a flow rate of 40 µL/min, with 400 s association time and 1,000 s dissociation time. After each injection, the sensor chip surface was regenerated by injecting 10 µL of 6M guanidium-HCl and 1M NaOH pH 11.0 mixed in a 4:1 ratio. All SPR data were analyzed using the BIA evaluation software 2.0.3 (GE Healthcare).

Animals

BALB/cAnNCrl and C57BL/6JCrl mice were purchased from Charles River, UK. Heterozygous IL-13eGFP mice were provided by Prof. Andrew McKenzie (20) and were bred in-house. Experiments were cage blocked: each cage contained one member of each group in the experiment, thus controlling for cage effects. Mouse accommodation and procedures were performed under UK Home Office licenses with institutional oversight performed by qualified veterinarians.

In vivo Alternaria model challenge

BALB/c mice were intranasally administered with 50 µg Alternaria allergen (Greer XPM1D3A25) and 10 µg HpARI1, HpARI2, or HpARI3 suspended in PBS, carried out under isoflurane anesthesia. Mice were culled 24 h later, and bronchoalveolar lavage (BAL) was collected (four lavages with 0.5 mL ice-cold PBS). Lungs were taken for single-cell preparation and flow cytometry, as previously described (15). Lung and BAL eosinophils were identified as SiglecF^{hi}CD11c^{-}CD45^{+} live cells. Lung ILC2 were identified as ICOS^{+}CD90.2^{+}Lineage^{-}CD45^{+} cells. IL-5 levels were quantified in undiluted BAL fluid by ELISA following the manufacturer's instructions (Invitrogen).

CMT-64 culture and treatment

CMT-64 cells (ECACC 10032301) were maintained in complete RPMI [RPMI 1640 medium containing 10% fetal bovine serum, 2 mM L-glutamine, 100 U/mL penicillin, and 100 µg/mL streptomycin (Thermo Fisher Scientific)] at 37°C, 5% CO_2; 96-well plates were seeded at 5×10^4 cells per well. Cells were grown to 100% confluency, washed, and incubated in complete RPMI containing HpARI2 or HpARI3 at the concentrations indicated. Cells were snap frozen on dry ice for at least 1 h, then thawed and incubated at 37°C as indicated, prior to the collection of supernatants and application to bone marrow cell cultures.

Bone marrow assay, ELISA, and flow cytometry

Bone marrow single-cell suspensions were prepared from C57BL/6 mice by flushing tibias and femurs with RPMI 1640 medium using a 21 g needle. Cells were resuspended in ACK lysis buffer (Gibco) for 5 min at room temperature, prior to resuspension in complete RPMI (with 10% FCS, 1% penicillin/streptomycin, 1% L-glutamine; Gibco) and passing through a 70 µm cell strainer. Cells were cultured in round-bottom 96-well plates in a final 200 µL volume, containing 0.5×10^6 cells/well. IL-2 and IL-7 (Biolegend) were added at a 10 ng/mL final concentration. CMT freeze-thaw supernatant prepared as described earlier was added at 50 µL per well. Cells were then cultured at 37°C, 5% CO2, for 5 days, prior to supernatant collection. IL-5 and IL-13 concentrations were assessed following the manufacturer's instructions using mouse-uncoated IL-5 and IL-13 enzyme linked immunosorbent assay (ELISA) kits (Invitrogen). For flow cytometry, after culture, cells were washed twice in PBS and stained with Zombie UV Fixable Viability Kit (Biolegend) according to the manufacturer instructions. Cells were then incubated for 30 min with anti-mouse CD16/CD32 (clone 93; Biologend) for Fc receptors blocking and were stained for CD45 (AF700, clone 30-F11; Biolegend), ICOS (PE, clone C398.4A; Biolegend), lineage markers (all on Pacific blue: CD3 clone 17A2, B220 clone RA3-6B2, CD5 clone 53–7.3, NK1.1 clone PK136, CD11b clone M1/70, and CD11c clone N418; Biolegend), CD25 (BV650, clone PC61; Biolegend), and ST2 (APC, clone RMST2-2; Invitrogen). Cells were then acquired on a LSR Fortressa (BD) and analyzed on FlowJo v10.9 (BD).

Assessment of ST2 binding by IL-33 in the presence of HpARI variants

Purified mST2 ectodomain (20 µM) was mixed individually with 40 µM of mIL-33, 25 µM HpARI2:mIL-33 and HpARI3:mIL-33 to a final volume of 200 µL. All samples were incubated for 1 h on ice and then applied to the Superdex S200 10/300 GL column (Cytiva) pre-equilibrated with buffer containing 20 mM Tris-Cl pH 8.0 and 100 mM NaCl. The eluted fractions were analyzed by SDS-PAGE.

Statistics

Data were analyzed using Graphpad Prism v10.0.0. When comparing independent groups, one-way analysis of variance (ANOVA) with Dunnett's posttest was used. When comparing groups over a timecourse, two-way ANOVA with Dunnett's posttest was used. Standard error of mean is used throughout. **** = $P < 0.0001$, *** = $P < 0.001$, ** = $P < 0.01$, * = $P < 0.05$, ns = not significant ($P > 0.05$).

RESULTS

H. polygyrus bakeri genome encodes three HpARI-like proteins

HpARI was identified by in-house transcriptomic and proteomic analysis of *Hpb* (15). Homology searching of published *Hpb* transcriptomic and genomic data via Wormbase ParaSite (21) identified a family of three HpARI genes from *Hpb*, all of which have the same characteristic domain organization of a secretory signal peptide followed by three complement control protein (CCP) domains (Fig. 1A). Proteomic analysis of HES showed that the most abundant HpARI family member was HPOL_0002204701 (intensity = 9×10^9), and so was named HpARI1, while the previously identified "HpARI" protein, HPBE_0000813301 (15), was renamed as HpARI2 (intensity = 1×10^9), and the final homologue with the lowest intensity in HES, HPBE_0002531401, was renamed HpARI3 (intensity = 4×10^7). Further analysis of a recent transcriptomic study of *Hpb* (22) showed that although HpARI1 and HpARI3 are expressed at a fairly consistent level throughout the lifecycle (albeit with HpARI3 at a far lower level compared to HpARI1), the expression of HpARI2 peaks early in infection (during the tissue-dwelling phase), with similar trends in males and females for each HpARI (Fig. 1B). The three HpARI family members show a high level of sequence similarity (69%–81% identity between the three HpARIs);

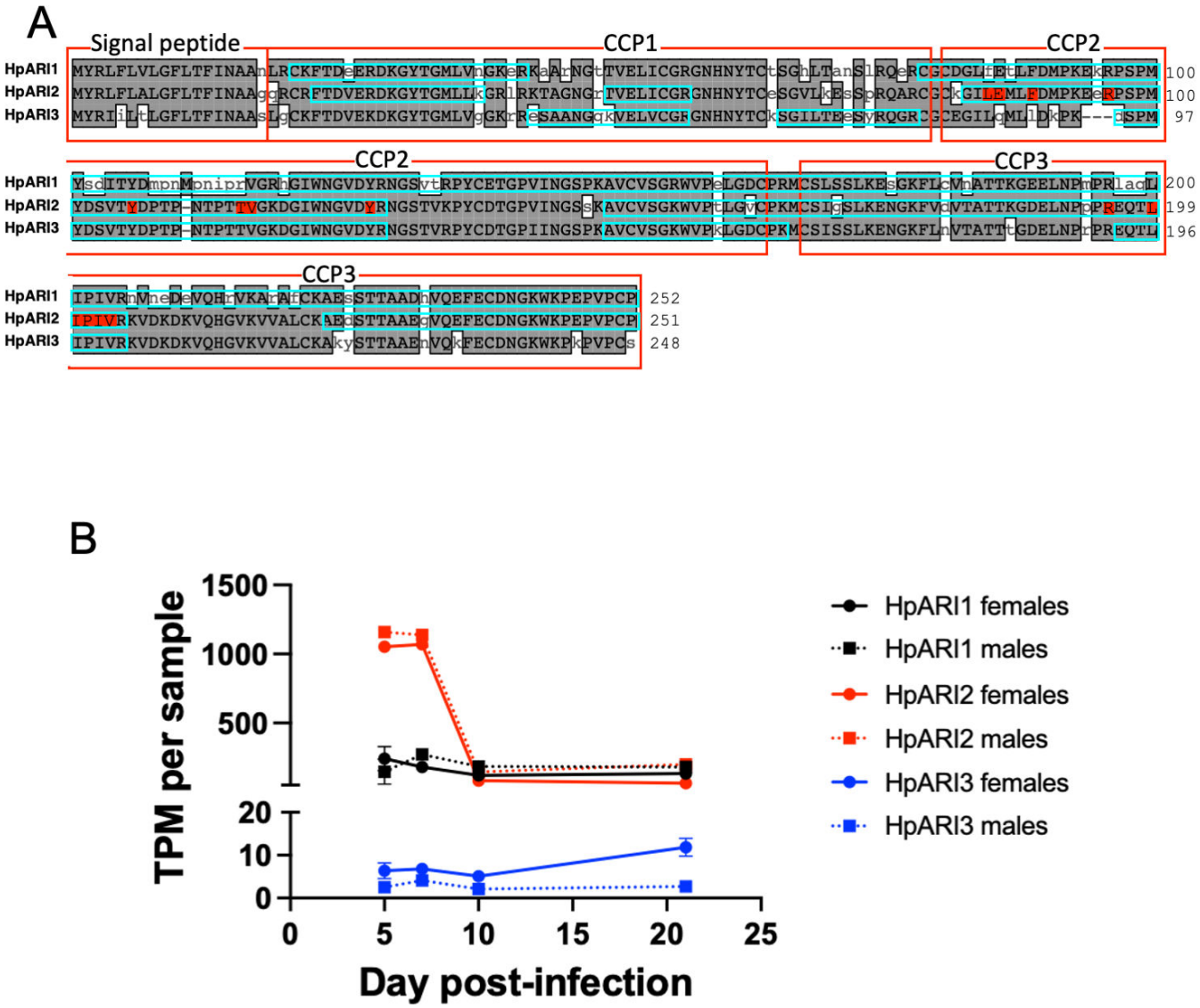

FIG 1 Sequences of HpARI family members. (A) Alignment of HpARI1, HpARI2, and HpARI3. Gray highlight indicates agreement with consensus. Signal peptide and CCP domains are indicated by red boxes, and coverage of peptides identified by mass spectrometry of HES is indicated by blue boxes. Residues in HpARI2-IL-33 interface are highlighted in red. (B) Transcripts per million (TPM) of HpARI1, HpARI2, and HpARI3 in male and female parasites over a timecourse of infection. Parasites were collected from four to nine mice per data point. Data retrieved from the Sequence Read Archive, PRJNA750155.

however, the HpARI3 sequence contains a notable three-amino acid deletion (at E94_R96 in HpARI2 sequence) at the N-terminal end of CCP2 (Fig. 1A), a region that contains an HpARI2-IL-33 interaction site (17).

The HpARI family members all bind IL-33 with sub-nanomolar affinities

The three HpARI family members were expressed in mammalian cells and purified for further testing. Each HpARI was added to the CMT-64 cells [which express high levels of IL-33 (15)], followed by freeze-thaw necrosis-induced IL-33 release. In this assay, all three proteins could suppress the IL-33 signal in a dose-dependent manner, indicating that they compete for IL-33 binding with the ELISA antibodies used for detection (Fig. 2A). HpARI3 required an approximately 8-fold higher concentration for IL-33 suppression (IC50 of HpARI1 and HpARI2 ~8 × 10^{-10} M, HpARI3 ~6 × 10^{-9} M). When binding affinity for IL-33 was tested by surface plasmon resonance, HpARI3 was likewise shown to have a

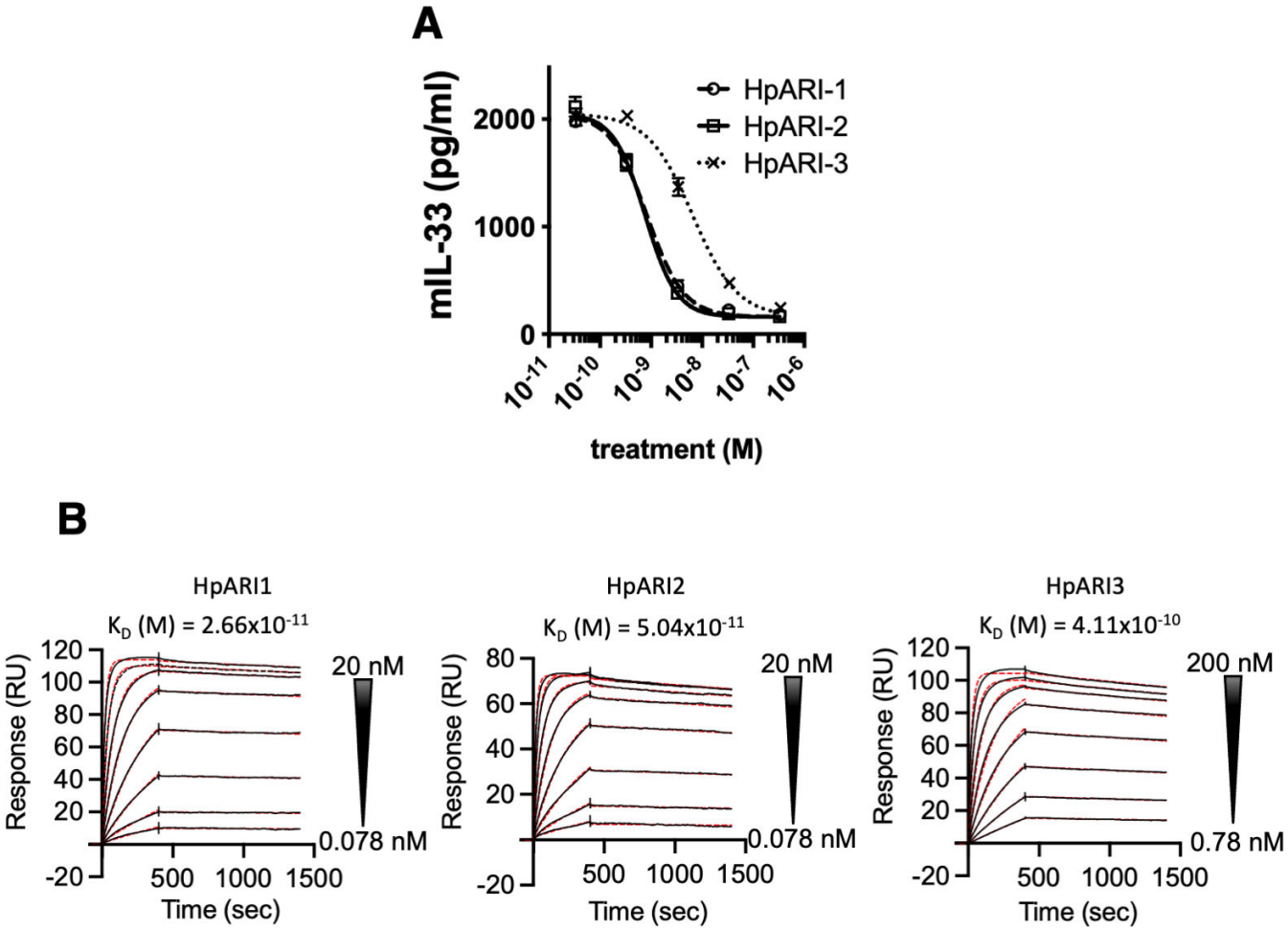

FIG 2 HpARI family members bind IL-33. (A) IL-33 detected in supernatant of CMT-64 cultures after freeze-thawing in the presence of HpARI1, HpARI2, or HpARI3. (B) Surface plasmon resonance (SPR) analysis of mouse IL-33 binding to chip-bound HpARI1, HpARI2 or HpARI3.

lower affinity for IL-33, albeit still with a sub-nanomolar K_D: HpARI1/2 has a K_D around 4×10^{-11} M, while HpARI3 has a K_D of 4×10^{-10} M (Fig. 2B).

HpARI family shows differing effects on IL-33-dependent responses *in vivo*

To test how each HpARI affected IL-33-dependent responses, we coadministered them intranasally to BALB/c mice with Alternaria allergen (a highly IL-33-dependent model [23–25]), and assessed type 2 innate lymphoid cell (ILC2) and eosinophil responses 24 h later (Fig. 3A). HpARI2 potently suppressed BAL and lung eosinophilia, ILC2 responses, and IL-5 release, as shown previously (15), while HpARI1 had a similar, albeit slightly blunted, suppressive effect (Fig. 3B through G). Surprisingly, HpARI3 had the opposite effect, amplifying responses in this model, with significantly increased lung eosinophilia and ILC2 activation (CD25 upregulation and increased cell size measured by FSC) as well as total IL-5 release (Fig. 3B through G). These increased responses in the presence of HpARI3 are remarkably similar to those seen with a truncation of HpARI2 lacking the CCP3 domain (HpARI_CCP1/2), which also amplifies IL-33 responses *in vivo* (7, 26). Although both the HpARI2 full-length protein and the HpARI_CCP1/2 truncation can bind to IL-33, only the HpARI2 full-length protein can block IL-33-ST2 interactions, while the HpARI_CCP1/2 cannot (26); therefore, we also tested the IL-33 blocking ability of HpARI3.

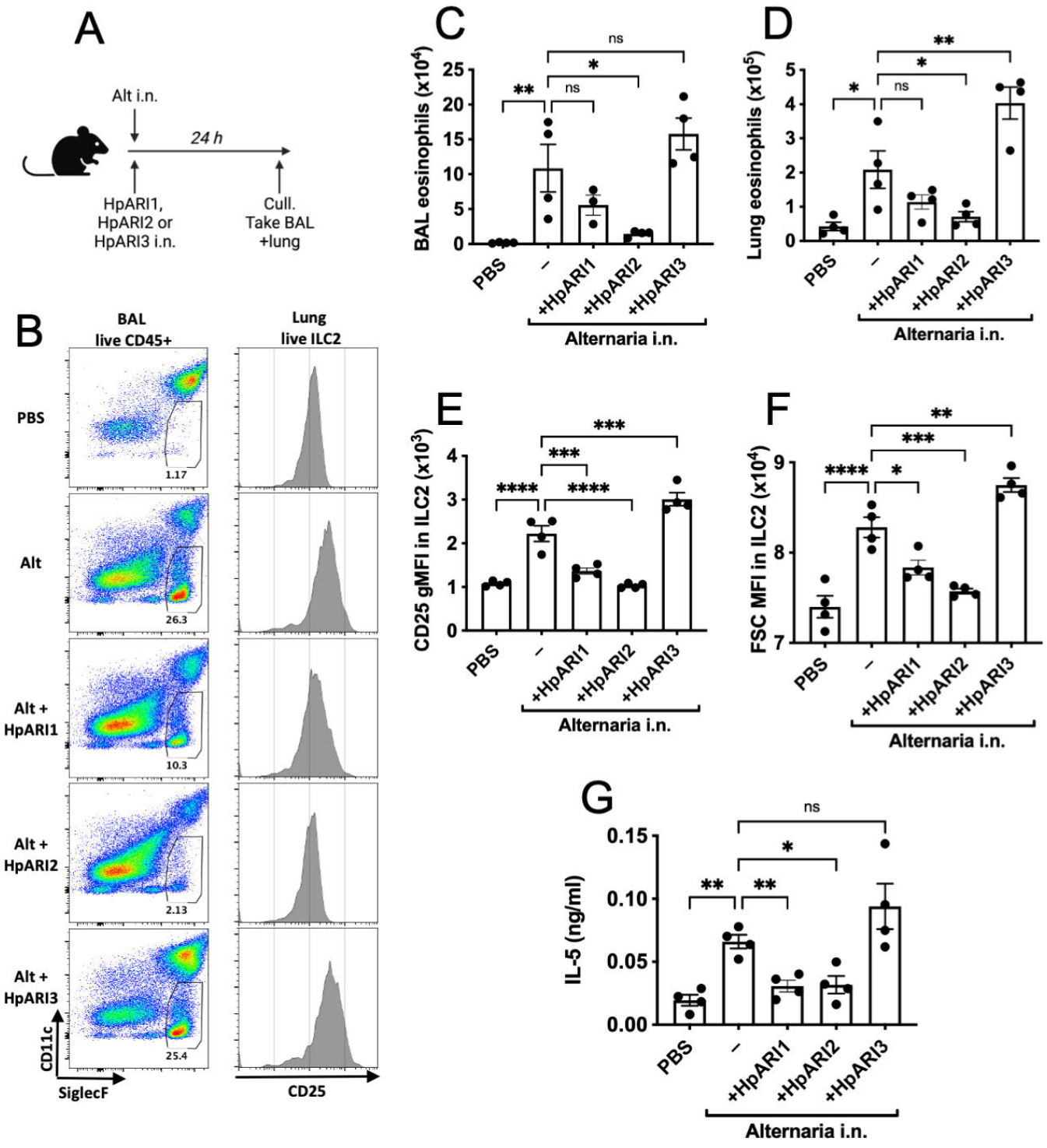

FIG 3 HpARI family members have differing effects against IL-33. (A) Experimental setup for B to G. HpARI1, HpARI2, or HpARI3 (10 µg) was coadministered with intranasal (i.n.) Alternaria allergen, and mice were culled 24 h later. (B) Flow cytometry of BAL Siglecf versus CD11c, gated on $CD45^+$ live cells, showing eosinophil gate (left). Flow cytometry of CD25 on lung ILC2, gated on live $ICOS^+CD90^+Lin^-CD45^+$ cells (right). Representative samples are shown. (C) Alternaria allergen was coadministered with HpARI1, HpARI2, or HpARI3 as shown in A, and BAL eosinophil numbers ($Siglecf^+CD11^-CD45^+$) measured 24 h later. (D) Eosinophil ($Siglecf^{hi}CD11^-CD45^+$) numbers in lung tissue. (E) CD25 expression level on lung ILC2 ($ICOS^+CD90^+Lin^-CD45^+$). (F) FSC mean in lung ILC2 ($ICOS^+CD90^+Lin^-CD45^+$) (G) IL-5 levels in cell-free BAL fluid. Data are representative of two repeat experiments with four mice per group. Error bars show SEM.

HpARI3 does not prevent IL-33 from binding to ST2

To determine whether different HpARI variants can prevent IL-33 from binding to ST2, we deployed a size exclusion chromatography (SEC) assay to assess IL-33-HpARI-ST2 complex formation (17). We first confirmed the formation of a complex of ST2 and IL-33 as the two proteins co-migrated as a higher molecular weight complex when compared with individual components (Fig. 4A). In contrast, as previously observed (17), the elution profile of ST2 was unaltered in the presence of HpARI2:mIL-33 complex, showing that

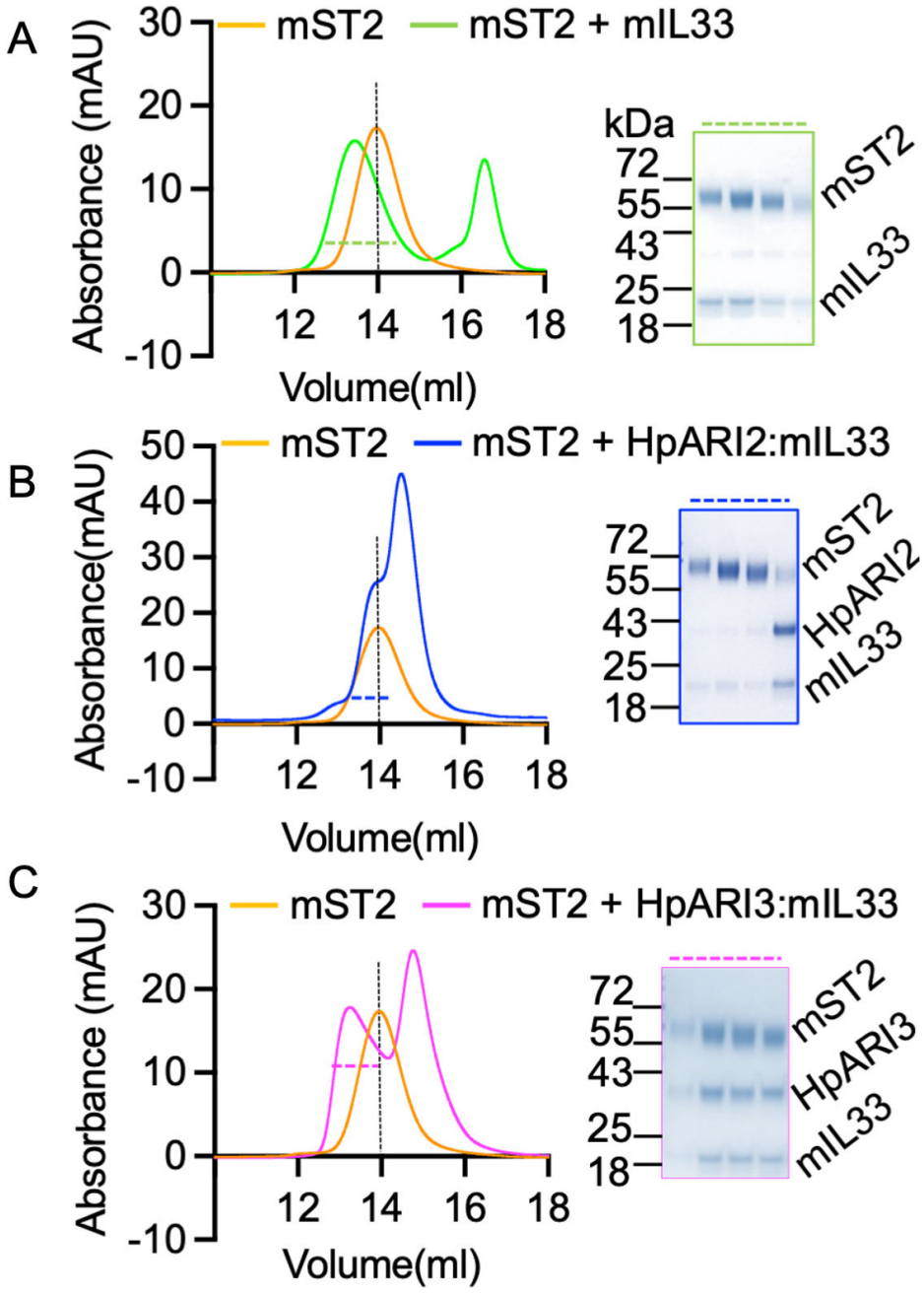

FIG 4 HpARI3 binding does not prevent IL-33-ST2 interaction. (A) SEC and SDS-PAGE analysis of purified mST2 ectodomain (orange curve) alone, or in the presence of mIL-33 (green). (B) SEC and SDS-PAGE analysis of purified mST2 ectodomain (orange curve) alone, or in the presence of HpARI2:mIL-33 (blue). (C) SEC and SDS-PAGE analysis of purified mST2 ectodomain (orange curve) alone, or in the presence of HpARI3:mIL-33 (magenta). SDS-PAGE analysis shows fractions indicated by dotted lines in SEC figures.

HpARI2 prevents IL-33 from binding to ST2 (Fig. 4B). In contrast, HpARI3 did not prevent IL-33 from binding to ST2 as indicated by elution peak shift in which ST2, IL-33, and HpARI3 co-elute, showing the formation of a complex containing all three components (Fig. 4C). Therefore, in contrast to HpARI2, HpARI3 interacts with IL-33 in a manner which does not prevent IL-33-ST2 interaction.

HpARI3 stabilizes IL-33

As HpARI3 cannot block IL-33-ST2 interactions, and instead amplifies responses in an IL-33-dependent model, we hypothesized that HpARI3 binding to IL-33 may stabilize the cytokine, extending its half-life. To test this, we used an *in vitro* IL-33 release and inactivation assay, which we developed previously (26). In this assay, CMT-64 cells are freeze-thawed to induce necrosis, and the released IL-33 is incubated at 37°C for between 15 min and 48 h after release to allow inactivation of the cytokine. Supernatants are subsequently applied to naïve IL-13eGFP murine bone marrow cells in the presence of IL-2 and IL-7 to support ILC2 differentiation, and ILC2 activation was assessed by flow cytometry for activation markers (IL-13eGFP and CD25 upregulation) and ELISA for secretion of IL-5 and IL-13. In medium control wells, CMT-64 freeze-thaw supernatants could only induce significant IL-5 and IL-13 production when applied within 6 h of thawing, indicating inactivation of IL-33 at later points of this timecourse, as shown previously (26). Conversely, CMT-64 cells freeze-thawed in the presence of HpARI2 could not induce any ILC2 activation due to blockade of released IL-33. In the presence of HpARI3, however, IL-33 in supernatants was able to stimulate high levels of IL-5 and IL-13 release and ILC2 activation (Fig. 5B through E), indicating strong IL-33 responses which were not inactivated even after incubation of IL-33-containing CMT-64 supernatants for 48 h at 37°C. The effects of HpARI3 were only evident in the presence of IL-33. HpARI3 alone did not activate ILC2, and the effects of HpARI3 to amplify IL-33-dependent ILC2 responses could be entirely abrogated by blockade of ST2 using HpBARI_Hom2 (Fig. 5F and G) (16).

Finally, to determine whether the effects of HpARI2 and HpARI3 could compete in combination, we added each HpARI at 1, 10, or 100 ng/mL to the CMT-64/ILC2 assay described earlier and measured released IL-5. Although sole HpARI3 treatment caused a dose-dependent increase in IL-5 release, HpARI2 caused a decrease, as expected. In combination, equivalent concentrations of each HpARI showed no significant change compared to the medium-only control, while an excess of HpARI2 significantly suppressed responses and an excess of HpARI3 significantly enhanced responses (Fig. 5H). Therefore, the suppression or enhancement of IL-33 responses *in vivo* by HpARI2 or HpARI3 will depend on the predominance of each molecule in the local milieu.

DISCUSSION

In this study, we describe a family of three HpARI proteins with high sequence similarity but differing effects on responses to IL-33. Although HpARI1 and HpARI2 suppress responses to IL-33, HpARI3 lacked the ability to prevent IL-33 from binding to ST2 and instead stabilized this highly labile cytokine in its active form, resulting in amplification of responses to IL-33 in *in vivo* and *in vitro* models.

The IL-33 activity-amplifying ability of HpARI3 was unexpected and would seem counterintuitive as total ST2-deficient mice are more susceptible to *Hpb* infection (6), implying the IL-33 pathway is largely helminth toxic. However, in addition to the well-described type 2 immunity-inducing effects of IL-33, recent publications have described a range of effects of IL-33 which can suppress type 2 immunity. IL-33 can activate and expand Foxp3$^+$ regulatory T cells (8), and in helminth infection, deletion of IL-33 in myeloid cells results in a defective regulatory T cell response, increased type 2 immunity, and accelerated helminth ejection (10). Furthermore, IL-33 can activate natural killer cell (27), Th1 (28) and CD8$^+$ T cell (9) IFN-γ production, potentially suppressing type 2 immunity. As both Th1/CD8$^+$ IFN-γ (29, 30) and Foxp3$^+$ regulatory T cell (31) responses

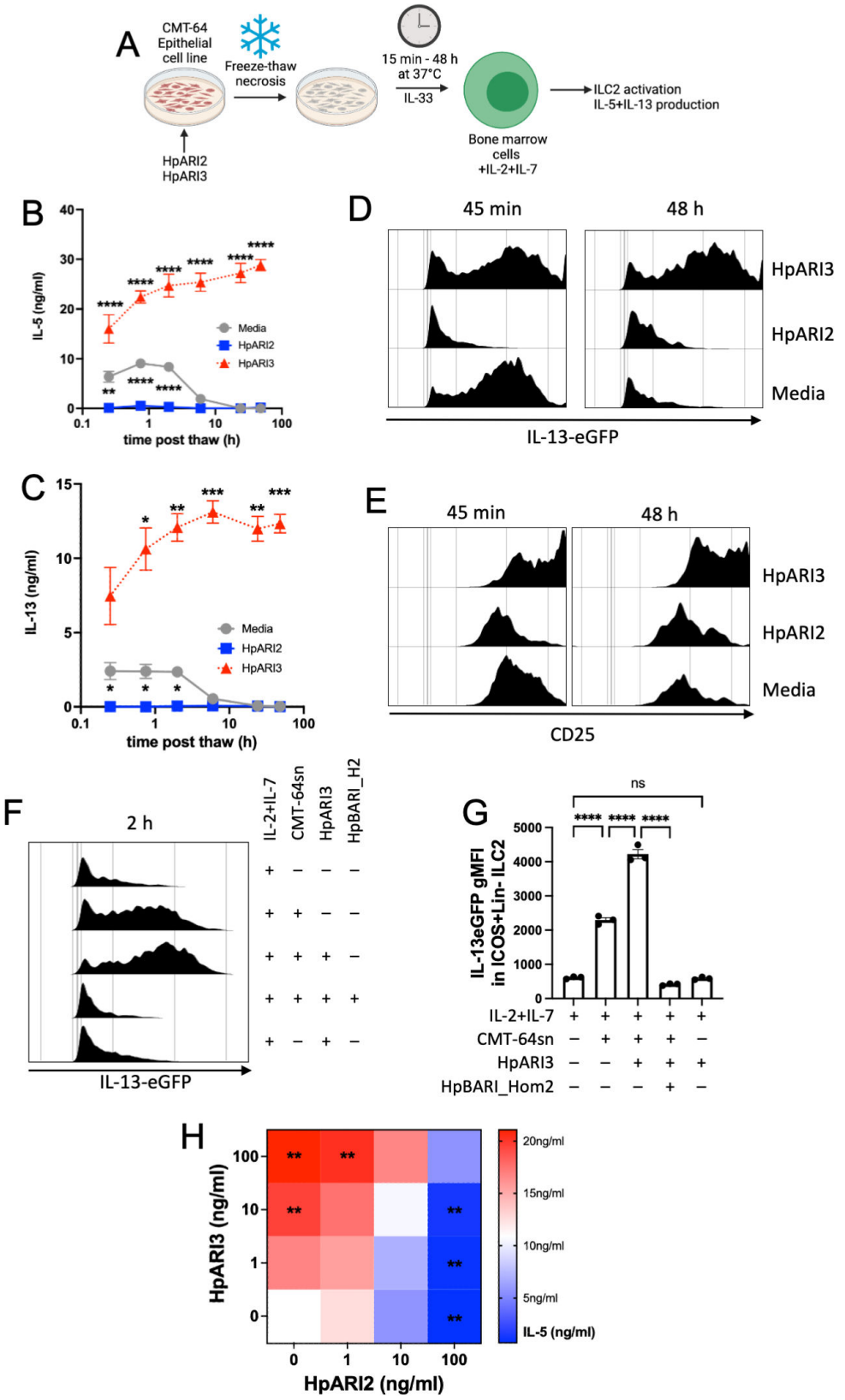

FIG 5 HpARI3 stabilizes IL-33 in its active form. (A) Experimental setup for B to G. Supernatants were taken over a timecourse after freeze-thawing of CMT-64 cells in the presence of HpARI2 or HpARI3, transferred to IL-13eGFP$^{+/-}$ bone marrow cells with IL-2 + IL-7, and cultured for 5 days. HpARI2 and HpARI3 were applied to CMT-64 cells at 10 µg/mL, then 50 µL of supernatants

(Continued on next page)

FIG 5 (Continued)

was added to a 200-µL bone marrow culture to give a final concentration of 2.5 µg/mL. Created with BioRender.com. (B) IL-5 levels in supernatants from cultures as shown in A, measured by ELISA. (C) IL-13 levels in supernatants from cultures as shown in A, measured by ELISA. (D) IL-13eGFP expression in gated $ICOS^+Lin^-CD45^+$ ILC2s from cultures as shown in A, measured by flow cytometry. (E) CD25 expression in gated $ICOS^+Lin^-CD45^+$ ILC2s from cultures as shown in A, measured by flow cytometry. Data from B to E representative of three repeat experiments. Error bar shows SEM of four technical replicates. Analyzed by a two-way ANOVA with Dunnett's posttest. (F) HpARI3 (100 ng/mL) and HpBARI_Hom2 (1,000 ng/mL) were applied to CMT-64 cells, prior to freeze-thaw, incubation at 37°C for 2 h, and transfer to cultures of bone marrow cells with IL-2 + IL-7 (or IL-2 + IL-7 alone), and cultured for 5 days. IL-13eGFP expression in gated $ICOS^+Lin^-CD45^+$ ILC2s was assessed by flow cytometry. Representative histograms are shown. (G) Geometric mean fluorescence intensity of IL-13eGFP in $ICOS^+Lin^-CD45^+$ ILC2s described in F. (H) HpARI2 and HpARI3 at a range of concentrations were applied to CMT-64 cells, prior to freeze-thaw, incubation at 37°C for 2 h, and transfer to cultures of bone marrow cells with IL-2 + IL-7, and cultured for 5 days. Levels of IL-5 in supernatants were measured by ELISA. Mean of three independent biological replicates. Statistical significance is shown as compared to the medium-only control. Analyzed by one-way ANOVA with Dunnett's posttest.

have been demonstrated to control type 2 immunity in *Hpb* infection, either of these pathways could be the target of HpARI3 responses.

Although HpARI3 expression was maintained at a lower level than that of HpARI1 or HpARI2, all three HpARI proteins were detectable in HES. Given that HpARI3 has a lower affinity for IL-33 than HpARI2, it might be expected that HpARI2's effects would dominate over HpARI3. However, in *in vitro* cultures, we found that HpARI2 and HpARI3 could compete in their effects, with equal concentrations of each HpARI resulting in no overall change in the response to IL-33, while an excess of HpARI2 resulted in a suppression and an excess of HpARI3 resulted in an amplification of the response to IL-33. Therefore, we hypothesize that differential timing or localization of HpARI protein release could determine the local HpARI2/HpARI3 ratio and therefore the resulting response to IL-33 during infection. IL-33's inflammatory versus immunosuppressive effects are partially controlled by the context of release: when IL-33 was deleted in epithelial cells, type 2 immunity and parasite ejection were deficient, while when IL-33 was deleted in myeloid cells, regulatory T cell responses were reduced, resulting in increased type 2 immunity and acerated parasite ejection (10). It would, therefore, be most advantageous for the parasite to block IL-33 in the local environment of the parasite during the early tissue-dwelling phase of infection (where necrotic damage to the epithelium is most likely), while IL-33 enhancement in the draining lymph node could amplify Th2-suppressive IFN-γ and regulatory T cell responses. Further work is required to investigate the roles of this family of immunomodulatory proteins during active infection.

ACKNOWLEDGMENTS

This work was funded by awards to H.J.M. from LONGFONDS|Accelerate as part of the AWWA project, the Medical Research Council (MR/S000593/1), and Wellcome (221914/Z/20/Z). We would like to acknowledge the support of Cara Henderson and Alan Score of the FingerPrints Proteomics Facility at the University of Dundee, which is supported by the "Wellcome Trust Technology Platform" award (097945/B/11/Z).

AUTHOR AFFILIATIONS

[1]Division of Cell Signalling and Immunology, School of Life Sciences, University of Dundee, Dundee, United Kingdom
[2]Department of Biology, University of York, York, United Kingdom
[3]Department of Biochemistry, University of Oxford, Oxford, United Kingdom
[4]Kavli Institute for Nanoscience Discovery and Dorothy Crowfoot Hodgkin Building, University of Oxford, Oxford, United Kingdom
[5]Department of Biological Sciences, Faculty of Science, University of Calgary, Calgary, Alberta, Canada

[6]Host-Parasite Interactions Research Training Network, University of Calgary, Calgary, Alberta, Canada
[7]Wellcome Centre for Integrative Parasitology, School of Infection and Immunity, University of Glasgow, Glasgow, United Kingdom
[8]Faculty of Veterinary Medicine, University of Calgary, Calgary, Alberta, Canada

AUTHOR ORCIDs

Abhishek Jamwal http://orcid.org/0009-0004-6842-6056
Constance A. M. Finney http://orcid.org/0000-0002-8459-8462
James D. Wasmuth http://orcid.org/0000-0002-9516-212X
Matthew K. Higgins http://orcid.org/0000-0002-2870-1955
Henry J. McSorley http://orcid.org/0000-0003-1300-7407

FUNDING

Funder	Grant(s)	Author(s)
Longfonds (Lung Foundation Netherlands)	Accelerate AWWA	Florent Colomb Henry J. McSorley
UKRI | Medical Research Council (MRC)	MR/S000593/1	Adefunke Ogunkanbi Henry J. McSorley
Wellcome Trust (WT)	221914/Z/20/Z	Florent Colomb Abhishek Jamwal Matthew K. Higgins Henry J. McSorley

AUTHOR CONTRIBUTIONS

Florent Colomb, Formal analysis, Investigation, Methodology, Writing – review and editing | Adefunke Ogunkanbi, Formal analysis, Investigation, Methodology, Writing – review and editing | Abhishek Jamwal, Formal analysis, Investigation, Methodology, Writing – review and editing | Beverly Dong, Investigation, Methodology | Rick M. Maizels, Methodology, Resources | Constance A. M. Finney, Methodology, Resources | James D. Wasmuth, Methodology, Resources | Matthew K. Higgins, Conceptualization, Formal analysis, Investigation, Methodology | Henry J. McSorley, Conceptualization, Data curation, Formal analysis, Funding acquisition, Investigation, Project administration, Supervision, Writing – original draft, Writing – review and editing

REFERENCES

1. McSorley HJ, Smyth DJ. 2021. IL-33: a central cytokine in helminth infections. Semin Immunol 53:101532. https://doi.org/10.1016/j.smim.2021.101532
2. Cohen ES, Scott IC, Majithiya JB, Rapley L, Kemp BP, England E, Rees DG, Overed-Sayer CL, Woods J, Bond NJ, et al. 2015. Oxidation of the alarmin IL-33 regulates ST2-dependent inflammation. Nat Commun 6:8327. https://doi.org/10.1038/ncomms9327
3. Moffatt MF, Gut IG, Demenais F, Strachan DP, Bouzigon E, Heath S, von Mutius E, Farrall M, Lathrop M, Cookson W, GABRIEL Consortium. 2010. A large-scale, consortium-based genomewide association study of asthma. N Engl J Med 363:1211–1221. https://doi.org/10.1056/NEJMoa0906312
4. Wechsler ME, Ruddy MK, Pavord ID, Israel E, Rabe KF, Ford LB, Maspero JF, Abdulai RM, Hu CC, Martincova R, Jessel A, Nivens MC, Amin N, Weinreich DM, Yancopoulos GD, Goulaouic H. 2021. Efficacy and safety of itepekimab in patients with moderate-to-severe asthma. N Engl J Med 385:1656–1668. https://doi.org/10.1056/NEJMoa2024257
5. Kelsen SG, Agache IO, Soong W, Israel E, Chupp GL, Cheung DS, Theess W, Yang X, Staton TL, Choy DF, Fong A, Dash A, Dolton M, Pappu R, Brightling CE. 2021. Astegolimab (anti-ST2) efficacy and safety in adults with severe asthma: a randomized clinical trial. J Allergy Clin Immunol 148:790–798. https://doi.org/10.1016/j.jaci.2021.03.044
6. Coakley G, McCaskill JL, Borger JG, Simbari F, Robertson E, Millar M, Harcus Y, McSorley HJ, Maizels RM, Buck AH. 2017. Extracellular vesicles from a helminth parasite suppress macrophage activation and constitute an effective vaccine for protective immunity. Cell Rep 19:1545–1557. https://doi.org/10.1016/j.celrep.2017.05.001
7. Meiners J, Reitz M, Rüdiger N, Turner J-E, Heepmann L, Rudolf L, Hartmann W, McSorley HJ, Breloer M. 2020. IL-33 facilitates rapid expulsion of the parasitic nematode *Strongyloides ratti* from the intestine via ILC2- and IL-9-driven mast cell activation. PLoS Pathog 16:e1009121. https://doi.org/10.1371/journal.ppat.1009121
8. Schiering C, Krausgruber T, Chomka A, Fröhlich A, Adelmann K, Wohlfert EA, Pott J, Griseri T, Bollrath J, Hegazy AN, Harrison OJ, Owens BMJ, Löhning M, Belkaid Y, Fallon PG, Powrie F. 2014. The alarmin IL-33 promotes regulatory T-cell function in the intestine. Nature 513:564–568. https://doi.org/10.1038/nature13577

9. Bonilla WV, Fröhlich A, Senn K, Kallert S, Fernandez M, Johnson S, Kreutzfeldt M, Hegazy AN, Schrick C, Fallon PG, Klemenz R, Nakae S, Adler H, Merkler D, Löhning M, Pinschewer DD. 2012. The alarmin interleukin-33 drives protective antiviral CD8(+) T cell responses. Science 335:984–989. https://doi.org/10.1126/science.1215418
10. Hung LY, Tanaka Y, Herbine K, Pastore C, Singh B, Ferguson A, Vora N, Douglas B, Zullo K, Behrens EM, Li Hui Tan T, Kohanski MA, Bryce P, Lin C, Kambayashi T, Reed DR, Brown BL, Cohen NA, Herbert DR. 2020. Cellular context of IL-33 expression dictates impact on anti-helminth immunity. Sci Immunol 5:eabc6259. https://doi.org/10.1126/sciimmunol.abc6259
11. Brooker S, Clements ACA, Bundy DAP. 2006. Global epidemiology, ecology and control of soil-transmitted helminth infections. Adv Parasitol 62:221–261. https://doi.org/10.1016/S0065-308X(05)62007-6
12. Hotez PJ, Brindley PJ, Bethony JM, King CH, Pearce EJ, Jacobson J. 2008. Helminth infections: the great neglected tropical diseases. J Clin Invest 118:1311–1321. https://doi.org/10.1172/JCI34261
13. Lothstein KE, Gause WC. 2021. Mining helminths for novel therapeutics. Trends Mol Med 27:345–364. https://doi.org/10.1016/j.molmed.2020.12.010
14. Maizels RM, McSorley HJ. 2016. Regulation of the host immune system by helminth parasites. J Allergy Clin Immunol 138:666–675. https://doi.org/10.1016/j.jaci.2016.07.007
15. Osbourn M, Soares DC, Vacca F, Cohen ES, Scott IC, Gregory WF, Smyth DJ, Toivakka M, Kemter AM, le Bihan T, Wear M, Hoving D, Filbey KJ, Hewitson JP, Henderson H, Gonzàlez-Cìscar A, Errington C, Vermeren S, Astier AL, Wallace WA, Schwarze J, Ivens AC, Maizels RM, McSorley HJ. 2017. HpARI protein secreted by a helminth parasite suppresses interleukin-33. Immunity 47:739–751. https://doi.org/10.1016/j.immuni.2017.09.015
16. Vacca F, Chauché C, Jamwal A, Hinchy EC, Heieis G, Webster H, Ogunkanbi A, Sekne Z, Gregory WF, Wear M, Perona-Wright G, Higgins MK, Nys JA, Cohen ES, McSorley HJ. 2020. A helminth-derived suppressor of ST2 blocks allergic responses. Elife 9:e54017. https://doi.org/10.7554/eLife.54017
17. Jamwal A, Colomb F, McSorley HJ, Higgins MK. 2023. Structural basis for IL-33 recognition and its antagonism by the helminth effector protein HpARI. bioRxiv. https://doi.org/10.1101/2023.08.10.552813
18. Johnston CJC, Robertson E, Harcus Y, Grainger JR, Coakley G, Smyth DJ, McSorley HJ, Maizels R. 2015. Cultivation of *Heligmosomoides polygyrus*: an immunomodulatory nematode parasite and its secreted products. J Vis Exp 98:e52412. https://doi.org/10.3791/52412
19. Doellinger J, Blumenscheit C, Schneider A, Lasch P. 2020. Isolation window optimization of data-independent acquisition using predicted libraries for deep and accurate proteome profiling. Anal Chem 92:12185–12192. https://doi.org/10.1021/acs.analchem.0c00994
20. Neill DR, Wong SH, Bellosi A, Flynn RJ, Daly M, Langford TKA, Bucks C, Kane CM, Fallon PG, Pannell R, Jolin HE, McKenzie ANJ. 2010. Nuocytes represent a new innate effector leukocyte that mediates type-2 immunity. Nature 464:1367–1370. https://doi.org/10.1038/nature08900
21. Howe KL, Bolt BJ, Shafie M, Kersey P, Berriman M. 2017. WormBase ParaSite - a comprehensive resource for helminth genomics. Mol Biochem Parasitol 215:2–10. https://doi.org/10.1016/j.molbiopara.2016.11.005
22. Pollo SMJ, Leon-Coria A, Liu H, Cruces-Gonzalez D, Finney CAM, Wasmuth JD. 2023. Transcriptional patterns of sexual dimorphism and in host developmental programs in the model parasitic nematode *Heligmosomoides bakeri*. Parasit Vectors 16:171. https://doi.org/10.1186/s13071-023-05785-2
23. Kouzaki H, Iijima K, Kobayashi T, O'Grady SM, Kita H. 2011. The danger signal, extracellular ATP, is a sensor for an airborne allergen and triggers IL-33 release and innate Th2-type responses. J Immunol 186:4375–4387. https://doi.org/10.4049/jimmunol.1003020
24. Bartemes KR, Iijima K, Kobayashi T, Kephart GM, McKenzie AN, Kita H. 2012. IL-33-responsive lineage- CD25+ CD44(hi) lymphoid cells mediate innate type 2 immunity and allergic inflammation in the lungs. J Immunol 188:1503–1513. https://doi.org/10.4049/jimmunol.1102832
25. McSorley HJ, Blair NF, Smith KA, McKenzie ANJ, Maizels RM. 2014. Blockade of IL-33 release and suppression of type 2 innate lymphoid cell responses by helminth secreted products in airway allergy. Mucosal Immunol 7:1068–1078. https://doi.org/10.1038/mi.2013.123
26. Chauché C, Vacca F, Chia SL, Richards J, Gregory WF, Ogunkanbi A, Wear M, McSorley HJ. 2020. A truncated form of HpARI stabilizes IL-33, amplifying responses to the cytokine. Front Immunol 11:1363. https://doi.org/10.3389/fimmu.2020.01363
27. Bourgeois E, Van LP, Samson M, Diem S, Barra A, Roga S, Gombert JM, Schneider E, Dy M, Gourdy P, Girard JP, Herbelin A. 2009. The pro-Th2 cytokine IL-33 directly interacts with invariant NKT and NK cells to induce IFN-gamma production. Eur J Immunol 39:1046–1055. https://doi.org/10.1002/eji.200838575
28. Komai-Koma M, Wang E, Kurowska-Stolarska M, Li D, McSharry C, Xu D. 2016. Interleukin-33 promoting Th1 lymphocyte differentiation dependents on IL-12. Immunobiology 221:412–417. https://doi.org/10.1016/j.imbio.2015.11.013
29. Filbey KJ, Grainger JR, Smith KA, Boon L, van Rooijen N, Harcus Y, Jenkins S, Hewitson JP, Maizels RM. 2014. Innate and adaptive type 2 immune cell responses in genetically controlled resistance to intestinal helminth infection. Immunol Cell Biol 92:436–448. https://doi.org/10.1038/icb.2013.109
30. Affinass N, Zhang H, Löhning M, Hartmann S, Rausch S. 2018. Manipulation of the balance between Th2 and Th2/1 hybrid cells affects parasite nematode fitness in mice. Eur J Immunol 48:1958–1964. https://doi.org/10.1002/eji.201847639
31. Smith KA, Filbey KJ, Reynolds LA, Hewitson JP, Harcus Y, Boon L, Sparwasser T, Hämmerling G, Maizels RM. 2016. Low-level regulatory T-cell activity is essential for functional type-2 effector immunity to expel gastrointestinal helminths. Mucosal Immunol 9:428–443. https://doi.org/10.1038/mi.2015.73